NEOPLASIA
www.neoplasia.com

Volume 17 Number 8 August 2015 pp. 634–649 634

EGFR Regulates the Development and Microarchitecture of Intratumoral Angiogenic Vasculature Capable of Sustaining Cancer Cell Intravasation

Petra Minder, Ewa Zajac, James P. Quigley and Elena I. Deryugina

The Department of Cell and Molecular Biology, The Scripps Research Institute, La Jolla, CA

Abstract

Many malignant characteristics of cancer cells are regulated through pathways induced by the tyrosine kinase activity of the epidermal growth factor receptor (EGFR). Herein, we show that besides directly affecting the biology of cancer cells *per se*, EGFR also regulates the primary tumor microenvironment. Specifically, our findings demonstrate that both the expression and signaling activity of EGFR are required for the induction of a distinct intratumoral vasculature capable of sustaining tumor cell intravasation, a critical rate-limiting step in the metastatic cascade. An intravasation-sustaining mode of intratumoral angiogenic vessels depends on high levels of tumor cell EGFR and the interplay between EGFR-regulated production of interleukin 8 by tumor cells, interleukin-8–induced influx of tumor-infiltrating neutrophils delivering their unique matrix metalloproteinase-9, and neutrophil matrix metalloproteinase-9–dependent release of the vascular permeability and endothelial growth factor, VEGF. Our data indicate that through VEGF-mediated disruption of endothelial layer integrity and increase of intratumoral vasculature permeability, EGFR activity significantly facilitates active intravasation of cancer cells. Therefore, this study unraveled an important but overlooked function of EGFR in cancer, namely, its ability to create an intravasation-sustaining microenvironment within the developing primary tumor by orchestrating several interrelated processes required for the initial steps of cancer metastasis through vascular routes. Our findings also suggest that EGFR-targeted therapies might be more effective when implemented in cancer patients with early-staged primary tumors containing a VEGF-dependent angiogenic vasculature. Accordingly, early EGFR inhibition combined with various anti-VEGF approaches could synergistically suppress tumor cell intravasation through inhibiting the highly permeable angiogenic vasculature induced by EGFR-overexpressing aggressive cancer cells.

Neoplasia (2015) 17, 634–649

Introduction

The epidermal growth factor receptor (EGFR) is a potent tyrosine kinase, which through downstream signaling networks regulates such basic cell functions as proliferation, chemotactic migration, invasion, and avoidance of apoptosis [1,2]. Elevated expression and constitutive activity of EGFR have been strongly associated with poor prognosis in many types of cancer, prompting the design of highly specific and potent EGFR inhibitors to control tumor growth and metastasis [3–5]. Those inhibitors include anti-EGFR monoclonal antibodies (mAbs) directed against the extracellular domain of the EGFR and small molecule tyrosine kinase inhibitors directed against the catalytic domain of the EGFR [6,7]. Currently, EGFR-targeted therapies are implemented or considered as an additional line of anticancer treatments in patients with non–small-cell lung cancer, pancreatic cancer, head and neck cancer, colorectal cancer, and malignant gliomas [8–13]. However, the somewhat modest clinical success of EGFR inhibitors [2,9,11,14–16] compared with their performance in

Address all correspondence to: Elena Deryugina, PhD, The Department of Cell and Molecular Biology, The Scripps Research Institute, La Jolla, CA 92037.
E-mail: deryugin@scripps.edu
Received 14 April 2015; Revised 28 July 2015; Accepted 10 August 2015

© 2015 The Authors. Published by Elsevier Inc. on behalf of Neoplasia Press, Inc. This is an open access article under the CC BY-NC-ND license (http://creativecommons.org/licenses/by-nc-nd/4.0/).
1476-5586
http://dx.doi.org/10.1016/j.neo.2015.08.002

preclinical models [17–23] suggests that, in addition to strongly fostering the malignant behavior of tumor cells, the enhanced activity of EGFR might also facilitate cancer progression by regulating the primary tumor microenvironment, especially during the early steps of tumor development and tumor dissemination.

Herein, we have proposed that besides direct regulation of tumor cell proliferation, migration and invasion, cancer cell–expressed EGFR can also regulate the production of distinct molecules involved in the establishment and modification of the tumor microenvironment. Among those molecules are vascular endothelial growth factor (VEGF), the major angiogenic factor [24,25], and interleukin 8 (IL-8), the major attractant for tumor-infiltrating neutrophils [26,27], the inflammatory cell type playing a critical early role in tumor angiogenesis and finally gaining the appreciation it deserves in cancer research [28–33]. Therefore, cancer cell–expressed EGFR can serve as an important regulator of tumor angiogenesis and angiogenesis-dependent tumor cell dissemination, including the intravasation step, i.e., the active entry of tumor cells into the vasculature.

In this study, we employed the high- and low-disseminating variants (hi/diss and lo/diss) of three distinct human tumor types, including HT-1080 fibrosarcoma, PC-3 prostate carcinoma, and HEp-3 head and neck carcinoma. The hi/diss and lo/diss variants of each tumor cell type possess similar tumorigenic and colonization capacities but manifest a substantial, 50- to 100-fold differential in their intravasation potential [34–37]. Notably, all three hi/diss variants express substantially higher levels of EGFR compared with the corresponding lo/diss counterparts, suggesting a specific role of EGFR in the intravasation process. By silencing EGFR in hi/diss tumor variants and comparing their fate in the spontaneous versus experimental metastasis models, we demonstrated the specific involvement of tumor cell EGFR in the *early* steps of the metastatic cascade. Furthermore, we showed that enhanced expression and activity of tumor cell EGFR contribute to spontaneous metastasis through facilitating the structural development of intratumoral angiogenic blood vessels required for the process of intravasation.

To functionally analyze the specific contribution of EGFR to intravasation, we used the HT-hi/diss cells in a microtumor model that uniquely allows to determine the actual numbers of intravasated tumor cells which escaped from the primary tumor and entered the circulation, and simultaneously to conduct quantitative analyses of the entire intratumoral vasculature of individual microtumors [37,38]. In this model, several microtumors are initiated from collagen-embedded tumor cells grafted on the highly vascularized chorioallantoic membrane (CAM) of chick embryos incubated *ex ovo*. In 4 to 5 days, robust angiogenic vasculature develops within growing CAM microtumors, facilitating intratumoral intravasation and vascular dissemination of aggressive cancer cells, which are quantified by a real-time polymerase chain reaction (PCR) in the distal portions of the CAM. Furthermore, the accessibility of CAM vessels for inoculations of fluorescent lectin to stain endothelial cells and for accurate injections of fluorescent dextrans to assess the permeability of tumor vasculature makes this model invaluable for quantification of intravasation along with the quantitative analyses of the microarchitecture and permeability of intratumoral vasculature [37,38]. In conjunction with the inhibition of EGFR expression or its activity, this microtumor model system has allowed us to demonstrate that EGFR regulates the efficiency of tumor cell intravasation and that EGFR activity determines such critical characteristics of the intratumoral angiogenic vessels as their microarchitecture and functional integrity.

In this study, we have illuminated a novel mechanism by which tumor cell EGFR mediates tumor cell dissemination through orchestrating the development of an intravasation-sustaining vasculature within the primary tumor. These EGFR-mediated induction and maintenance of intratumoral angiogenic vessels permeable for tumor cells involve IL-8–induced influx of tumor-infiltrating neutrophils delivering a unique form of matrix metalloproteinase (MMP)-9, known to catalytically release angiogenesis-inducing VEGF, which is also a powerful regulator of vascular permeability. Therefore, our study has established an important link between the enhanced activity of EGFR in human tumor cells possessing high dissemination potential and the EGFR-induced molecular cross talk between IL-8, neutrophil MMP-9, and MMP-9–released VEGF, evoking within the primary tumor the development of a distinct, intravasation-sustaining vasculature.

Materials and Methods

Reagents

Rabbit antibodies specific for human EGFR (2646) and phospho-EGFR at Y1068 (1727-1) were purchased from Cell Signaling Technology Inc. (Danvers, MA) and Epitomics (Burlingame, CA), respectively. Anti-human MMP-9 murine mAbs were generated in our laboratory. Anti-tubulin mouse mAb 10D8 was from Biolegend (San Diego, CA). Horseradish peroxidase–conjugated anti-rabbit antibody (115-000-003) and anti-mouse antibody (115-035-003) were obtained from Jackson Laboratory (Sacramento, CA). EGFR-specific tyrosine kinase inhibitor erlotinib (sc-202154) was purchased from Santa Cruz (Dallas, TX). Recombinant human VEGF (AF-100-20A) was obtained from Peprotech (Rocky Hill, NJ). Human neutrophil MMP-9 was purified as described [39].

Cell Lines and Culture Conditions

HT-lo/diss and HT-hi/diss variants were generated by *in vivo* selection for correspondingly low and high levels of intravasation [34] from the original human fibrosarcoma HT-1080 cell line (ATCC, Manasass, VA). The HT-hi/diss cells were additionally transfected with GFP. HEp-hi/diss cells are derivatives of the original human head and neck epidermoid carcinoma, HEp-3, initially described in [40] and recently in [37]. PC-hi/diss cells have been generated from the original human prostate carcinoma cell line PC-3 as described [36]. Cells were cultured in Dulbecco's modified Eagle's medium (DMEM) supplemented with 10% FBS (D-10).

EGFR Silencing and Inhibition of EGFR Activity

Small interfering RNA (siRNA) against human EGFR (a pool of three EGFR-specific constructs, sc-29301) and nonsilencing control siRNA (sc-37007) were purchased from Santa Cruz (Dallas, TX). The day before siRNA transfection, the cells were plated in D-10 without antibiotics at concentrations resulting in 70% to 80% confluence the following day. Transfections were performed with 50 nM siRNA and Lipofectamine 2000 or RNAiMax (Life Technologies, Grand Island, NY), according to the manufacturer's instructions. After an overnight incubation, the siRNA-treated cells were detached, washed in D-10 and serum-free-DMEM, resuspended in serum-free-DMEM, and used in the various assays. EGFR activity was inhibited by erlotinib, which was added to tumor cells or primary microtumors at a final concentration of 30 μM.

Quantitative Real-Time Reverse Transcription PCR (qRT-PCR)

Relative expression levels of genes for EGFR, VEGF, and IL-8 were determined by qRT-PCR. Total RNA was extracted from the cells

with TRIzol (Invitrogen), and 2 μg of isolated RNA was reverse-transcribed using the RNA to cDNA EcoDry Premix (639549; Clontech, Mountain View, CA). The resulting cDNA was analyzed by qRT-PCR in an iCycler iQ (Bio-Rad). Each reaction contained 60 ng of cDNA as template, LightCycler 480 SYBR Green Master Mix (04707516001; Roche, San Francisco, CA), and each of forward and reverse primers used at 0.4 μM. PCR conditions included heating for 5 minutes at 95°C, followed by 40 cycles of 30 seconds at 95°C, 30 seconds at 60°C, and 60 seconds at 72°C. The primer sequences are as follows:

GAPDH: 5 -ACTGCTAGCCGCTTCTTCTT-3 (forward),
5 -GACAAGCTTCCCGTTCTCAG-3 (reverse);
EGFR: 5 -AGGCAGGAGTAACAAGCTCAC-3 (forward),
5 -ATGAGGACATAACAAGCCACC-3 (reverse);
VEGF: 5 -CGAAACCATGAACTTTCTGC-3 (forward),
5 -CCTCAGTGGGCACACACTCC-3 (reverse);
IL8: 5 -AGGGTTGCCAGATGCAATAC-3 (forward),
5 -CCTTGGCCTCAATTTTGCTA-3 (reverse).

A melt curve analysis was performed to ensure specific amplification. For each target gene, relative levels of expression were normalized against housekeeping gene signal, GAPDH, generating Δ cycle threshold (Ct) value (ΔCt = Ct target gene − Ct reference gene) [41]. The relative gene expression was calculated according to the formula $2^{-\Delta\Delta Ct}$, where ΔΔCt = ΔCt experimental setting − ΔCt control setting [42].

Animal Models

All experiments involving live animals were performed in accordance of animal protocol approved by The Scripps Research Institute Animal Care and Use Committee.

Spontaneous Intravasation Model

The chick embryo spontaneous metastasis model was conducted as described [34,35]. On day 10 of incubation, HT-1080 and HEp-3 tumor variants were grafted at 4×10^5 to 5×10^5 cells, and PC-3 tumor variants were grafted at 2×10^6 cells per chick embryo. To compensate for reduced levels of cell proliferation after EGFR silencing, the siEGFR-treated cells were used at 1.3× excess over control cells. After 5 days (HT-1080 and HEp-3 cells) or 7 days (PC-3 cells), the primary tumors were excised and weighed. To determine the numbers of intravasated tumor cells, portions of the distal CAM were harvested 2 to 3 cm from the edge of the primary tumor, a distance that is far too great to represent a stromal migration route for escaping primary tumor cells. Instead, primary tumor cells arrest in the CAM vasculature after they actively have entered the angiogenic vessels at the primary tumor site. Therefore, the tumor cells in the distal CAM represent the intravasated cells that have disseminated through the vascular routes.

In the case of GFP-labeled cells (e.g., HT-hi/diss cells), the intravasated cells that had disseminated from the primary tumors could be visualized in the distal CAM by epifluorescent microscopy after highlighting CAM vasculature with Rhodamine-conjugated *Lens culinaris* agglutinin (LCA; Vector Labs, Burlingame, CA; 25 μg per embryo). The intravasated cells could be seen as intact cells at different stages of progression from leaving the CAM vasculature towards entering the CAM mesoderm (Supplementary Figure S1). The majority of intravasated cells are visualized as single cells because spontaneous intravasation occurs through the angiogenic vasculature that requires some time for development and, therefore, the first sizable wave of intravasation occurs on day 4 after cell grafting, leaving little time for proliferation of tumor cells after their extravasation from the CAM capillaries into the distal CAM stroma. However, the actual numbers of intravasated cells are relatively low, making their quantification by microscopy inefficient and statistically unreliable. Therefore, the levels of intravasation were quantified by extremely sensitive qPCR detecting human-specific *Alu* repeats, the method that has been originally introduced in [43] and extensively used with modifications in our studies [34,36,37,44,45].

Experimental Metastasis Model

Vascular arrest and tissue colonization assays were performed as described [35,46]. Tumor cells (5×10^4) were injected directly into the allantoic vein of chick embryos developing *in ovo*. Because of the particularities of blood circulation in the avian embryo, intravenously (i.v.) inoculated cells are trapped back in the vascular networks of the CAM, where GFP-tagged tumor cells could be visualized by epifluorescent microscopy against LCA-contrasted CAM vessels. After 5 days, i.v. injected tumor cells form multicellular colonies within CAM stroma, characteristic of metastatic outgrowths (Supplementary Figure S2). This robust colony formation is in clear contrast to the single cell status of cells that have spontaneously intravasated at the primary tumor site and rapidly arrested in the CAM capillary system (Supplementary Figure S1). To quantify the levels of vascular arrest and colonization, portions of the CAM were analyzed by quantitative *Alu*-qPCR correspondingly at 2 hours and 5 days after cell inoculations.

CAM Microtumor Model

This model is based on the generation of multiple microtumors developing on the CAM of chicken embryos incubated *ex ovo*, allowing for quantitative analyses of primary tumors as whole units (micro-organs) [37,38]. The GFP-labeled HT-hi/diss cells, non-treated or transfected with control or EGFR siRNA constructs, were mixed with 2.2 mg/ml neutralized type I collagen (Becton Dickinson, Bedford, MA). Nontreated and siCtrl-treated cells were used at 1×10^7 cells/ml, whereas siEGFR- and erlotinib-treated cells were used at 1.3×10^7 cells/ml. Five 10-μl aliquots of cell-containing collagen mixtures were placed separately on the top of the CAM of 10-day-old embryos developing *ex ovo* (Supplementary Figure S3). Where indicated, developing microtumors were treated daily by topical applications of erlotinib (30 μM), VEGF (250 ng/ml), or purified human neutrophil proMMP-9 (1 μg/ml) delivered in 10 μl of PBS supplemented with 1% DMSO (vehicle). After 5 days, Rhodamine-conjugated LCA was inoculated i.v. to highlight the vasculature (25 μg per embryo). Within 5 to 10 minutes, microtumors were visualized using an Axio Imager (Carl Zeiss, Germany) and images were acquired with Axiovision Rel. 4.6 software (Carl Zeiss). Acquisition of 5-μm-thick *z*-stacks of intratumoral areas allowed us to confirm that the LCA-highlighted blood vessels indeed were localized within the primary microtumor, as they are surrounded by GFP-labeled tumor cells within a single optical z-stack (Supplementary Figure S4). For the size distribution analysis of intratumoral blood vessels, lumen diameters were quantified using CS5 Adobe Photoshop software in the images taken at the original magnification of 200× (20× objective × 10× eyepiece). The numerical data were graphically presented using GraphPad Prism (GraphPad, San Diego, CA). To determine the level of

neutrophil influx, microtumors were excised and frozen, and tumor sections were immunofluorescently stained for neutrophils. Because the neutrophils are the major cellular source of MMP-9 in the avian [44,45] as well as in mammalian species [47], chick embryo neutrophils were stained as described [39] with an anti-chicken MMP-9 mAb generated in our laboratory. The neutrophilic identity of MMP-9–positive cells was confirmed by their characteristic multilobed nuclei stained with DAPI.

Quantitative Alu-PCR Analysis (Alu-qPCR)

Quantification of disseminated human tumor cells in chick embryo CAM was performed with quantitative real-time PCR assay originally established in the L. Ossowski laboratory [43] and subsequently used by us with some modifications [34,36,37,45,48]. This assay is based on the quantification of human-specific *Alu* sequence repeats in total DNA extracted from the host tissue. Briefly, genomic DNA was extracted from the CAM tissue using the Puregene DNA purification system (Qiagen, Minneapolis, MN). *Alu*-qPCR was performed to amplify primate-specific *Alu* repeat sequences using 10 ng of genomic DNA as a template in a Bio-RadMyIQLightCycler (Bio-Rad, Hercules, CA). The dsDNA binding dye SYBR green (Life technologies, Grand Island, NY) was used for quantification of human tumor cells. The Ct values were converted into numbers of human cells using a standard curve generated by spiking constant numbers of chicken cells with serially diluted human tumor cells.

Measurement of Vascular Permeability

CAM microtumors were generated from unlabeled HT-hi/diss cells. On day 5, embryos were inoculated with low mol. wt., permeable, tetramethylrhodamine (TRITC)-conjugated 155-kDa dextran (Sigma, Saint Louis, MO). After 1 hour, high mol. wt., nonpermeable, fluorescein isothiocyanate (FITC)–conjugated, 2000-kDa dextran (Sigma) was inoculated to displace the permeable dextran and provide means to measure the total volume of intratumoral vasculature. Microtumors and intratumoral vasculature were imaged at fixed exposure times. Then, microtumors were excised and lysed in 0.3-ml modified radioimmunoprecipitation assay (RIPA) buffer. Red fluorescence was measured at 576 nm, providing amounts of tissue-retained permeable TRITC-dextran. Green fluorescence emitted by FITC-dextran was measured at 516 nm, providing the volume of perfusable vasculature. Red-to-green fluorescence ratios were determined for individual microtumors to provide quantification of vascular permeability independent of total volume of intratumoral vasculature.

Western Blot Analyses and ELISA

Cells were lysed in modified RIPA buffer in the presence of protease inhibitors. Primary tumors were excised from the CAM, snap-frozen in liquid nitrogen and ground, and proteins were extracted in PBS. Protein concentration was determined using the BCA protein assay from Pierce (Thermo Scientific, Rockford, IL). To analyze EGFR and pEGFR expression, equal amounts of protein (20 μg/lane) were reduced and separated on 4% to 20% Tris-glycine sodium dodecyl sulfate polyacrylamide gel electrophoresis gels (Life Technologies). After protein transfer, the membranes were blocked in TBS-Tween 20 containing 5% milk and probed with primary antibodies. Membranes were incubated with secondary HRP-conjugated antibodies, and immunoreactive bands were visualized using SuperSignal West Pico Chemiluminescent Substrate (Pierce). The levels of human VEGF and human IL-8 were analyzed by capture ELISA kits from Peprotech (900-M10 and 900-M18, respectively), according to the manufacturer's instructions. We have also established that these ELISA kits do not detect any chicken VEGF or chicken IL-8–like cytokine.

Statistical Analysis

Data processing was conducted using GraphPad Prism. The data are presented as means ± SEM of percentage changes or fold differences calculated from the pooled data of independent experiments in which each individual data point was compared with the mean of corresponding control. Statistical significance was evaluated using two-tailed unpaired Student *t* test for $P < .05$. *P* values of $<.05$, $<.01$, and $<.001$ are indicated by *, **, and ***, respectively.

Results

Positive Correlation between Tumor Cell Intravasation and EGFR Expression

The functional role of EGFR in the early steps of metastasis was investigated by using hi/diss and lo/diss variants of human HT-1080 fibrosarcoma, HEp-3 head and neck carcinoma, and PC-3 prostate carcinoma, all of which were selected *in vivo* for a substantial differential in intravasation capacity [34,36,37]. When levels of tumor cell intravasation were compared for primary tumors of similar size (Figure 1*A*), the lo/diss variants demonstrated much lower (HEp-lo/diss) or almost no ability (HT-lo/diss and PC-lo/diss) to enter into the CAM vasculature retaive to their hi/diss counterparts (Figure 1*B*). Notably, when probed for EGFR expression, all three hi/diss tumor variants demonstrated approximately five-fold more EGFR protein as compared with their respective lo/diss variants (Figure 1*C*). Together, these data suggested a functional link between EGFR expression and spontaneous tumor cell dissemination.

Functional Involvement of EGFR in the Early Steps of the Metastatic Cascade

To verify that EGFR might regulate tumor cell intravasation, EGFR expression was downregulated in the hi/diss variants with EGFR siRNA (siEGFR). Efficient silencing of EGFR gene in all three tumor types was confirmed in comparison with control siRNA (siCtrl) by qRT-PCR (Figure 2*A*). Furthermore, Western blot analysis confirmed the prolonged downregulation of EGFR expression at the protein level (Figure 2*B*). The deep and sustained suppression of EGFR protein (up to and beyond 5 days) allowed us to use the relatively short-term chick embryo metastasis models to investigate whether EGFR is functionally involved in specific steps of the metastatic cascade, namely, in the intravasation step in the spontaneous metastasis model and in tissue colonization in the experimental metastasis model.

In agreement with the known regulatory effects of EGFR on cell proliferation, downregulation of EGFR resulted in a 20% to 25% decrease in tumor growth *in vivo* (data not shown). Therefore, to compensate for this modestly reduced proliferation, the siEGFR-treated cells were used at 1.3-fold excess over control cells in the spontaneous metastasis model, allowing for generation of primary tumors of similar sizes and for separation of the overall effects of EGFR silencing on tumor growth from its specific effects on tumor cell intravasation. Despite similar sizes of primary tumors developed from siCtrl- and siEGFR-treated cells (Figure 2*C*), EGFR silencing (performed with two different sets of siRNA constructs against EGFR

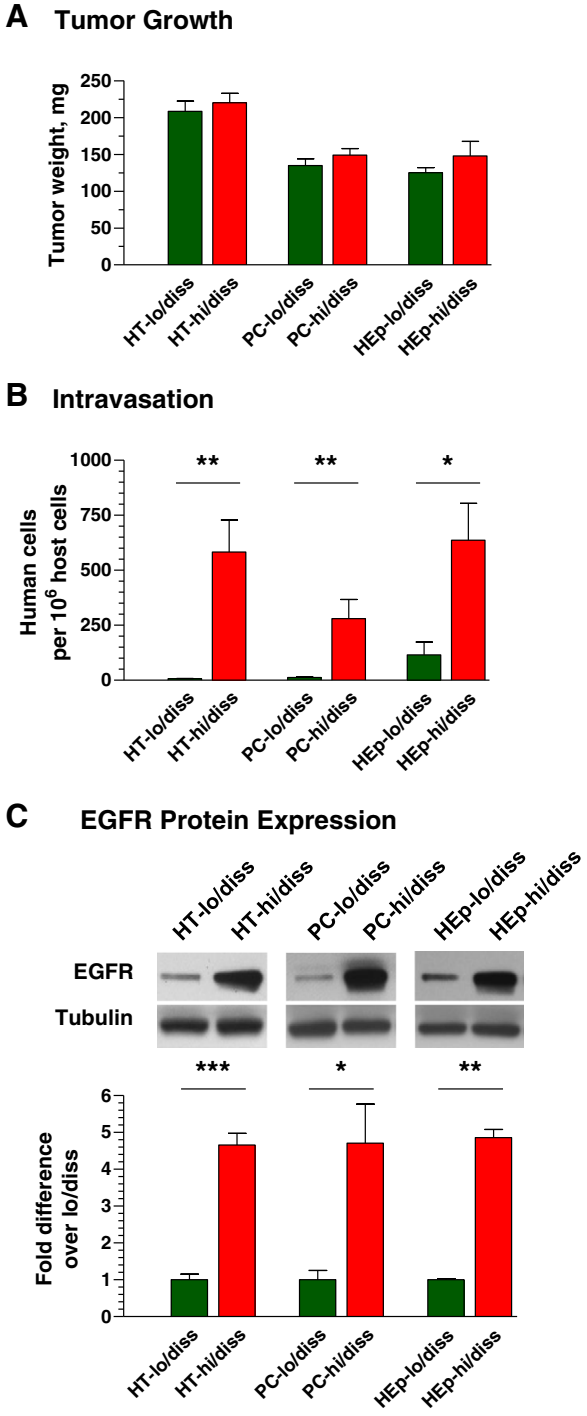

Figure 1. High levels of tumor cell intravasation correlate with EGFR overexpression. (A) On day 5 (HT-1080 and HEp-3 variants) or day 7 (PC-3 variants) after cell grafting, primary tumors were excised and weighed. (B) Tumor cell intravasation was quantified by *Alu*-qPCR for embryos bearing tumors of similar size. (C) Cell lysates were analyzed for total EGFR protein by Western blotting. (Bar graph) Densitometry of EGFR expression relative to alpha-tubulin (loading control).

transcripts) caused a significant, from 65% to 90%, reduction in intravasation levels in all three hi/diss tumor types (Figure 2*D*). Thus, the ability of tumor cells to disseminate from the primary tumor through vascular routes positively correlated with the levels of EGFR expression.

In contrast to the spontaneous metastasis model, no significant effects of EGFR knockdown were observed in the experimental metastasis model, where tumor cells are inoculated directly into the circulation, thereby bypassing the early steps of the metastatic cascade. Downregulation of EGFR produced no significant effects on vascular arrest of HT-hi/diss cells as measured 2 hours after cell inoculations (Figure 2*E*), indicating that EGFR did not affect the initial retention of this tumor type in the capillary network of the CAM. In addition, no significant differences were observed in 5-day tissue colonization by siCtrl- and siEGFR-treated HT-hi/diss cells (Figure 2*E*). In a similar fashion, EGFR silencing did not affect either vascular arrest or CAM colonization of PC-hi/diss or HEp-hi/diss cells (data not shown). This clear lack of major effects of siRNA treatments on the late stages of tumor metastasis, i.e., arrest, extravasation, and tissue colonization, allowed us to exclude major off-target effects of the siRNA constructs and to conclude that EGFR might functionally and specifically regulate an early step of the metastatic cascade, namely, intravasation, which in turn critically depends on the establishment of tumor-induced angiogenic vasculature.

EGFR and Development of Intravasation-Sustaining Angiogenic Vasculature

Because our data suggested that EGFR mechanistically regulates the ability of tumor cells to spontaneously disseminate through vascular routes, we investigated whether the negative effect of EGFR silencing on intravasation could be attributed to specific changes in tumor angiogenesis. To address this possibility, we used a modified spontaneous metastasis model involving generation of multiple CAM microtumors. An extensive neovasculature rapidly develops within these microtumors, thereby facilitating the process of tumor cell intravasation. The levels of intravasation are determined in the distal CAM by *Alu*-qPCR, whereas microtumors are analyzed in their entirety for the microarchitecture and permeability of their angiogenic vasculature by epifluorescent microscopy [37,38].

CAM microtumors of similar size were generated from GFP-tagged HT-hi/diss cells transfected with control or EGFR siRNA (Supplementary Figure S3), allowing for quantitative comparisons between two types of treatment. On day 5, epifluorescence microscopy of microtumors demonstrated that both control and EGFR-silenced cells triggered strong vascular responses and attracted comparable numbers of blood vessels converging onto the border of primary microtumors (Figure 3*A, left*). However, angiogenic vasculature analyzed within the tumors at a higher magnification indicated substantial differences in vessel microarchitecture. Thus, the vasculature within control microtumors showed well-defined networks of lumen-containing blood vessels, whereas EGFR-deficient microtumors displayed poorly perfused vessels, leading to an impression of a somewhat less vascularized tumor interior (Figure 3*A, middle and right*). However, quantitative analysis indicated almost equivalent blood vessel density inside both types of microtumors (Figure 3*B*). Interestingly, whereas no differences were observed in larger vessels (30-50 μm in size), control and siEGFR-deficient tumors manifested a significant differential in vessels with lumens <30 μm (Figure 3*C*). Thus, 60% of blood vessels within control tumors had lumens with a diameter between 15 and 30 μm compared with only 28% of such vessels in EGFR-deficient tumors. Reciprocally, 54% of vessels formed within microtumors developing from siEGFR-treated tumor cells had a lumen diameter of <15 μm, whereas this very thin vessel category was represented by

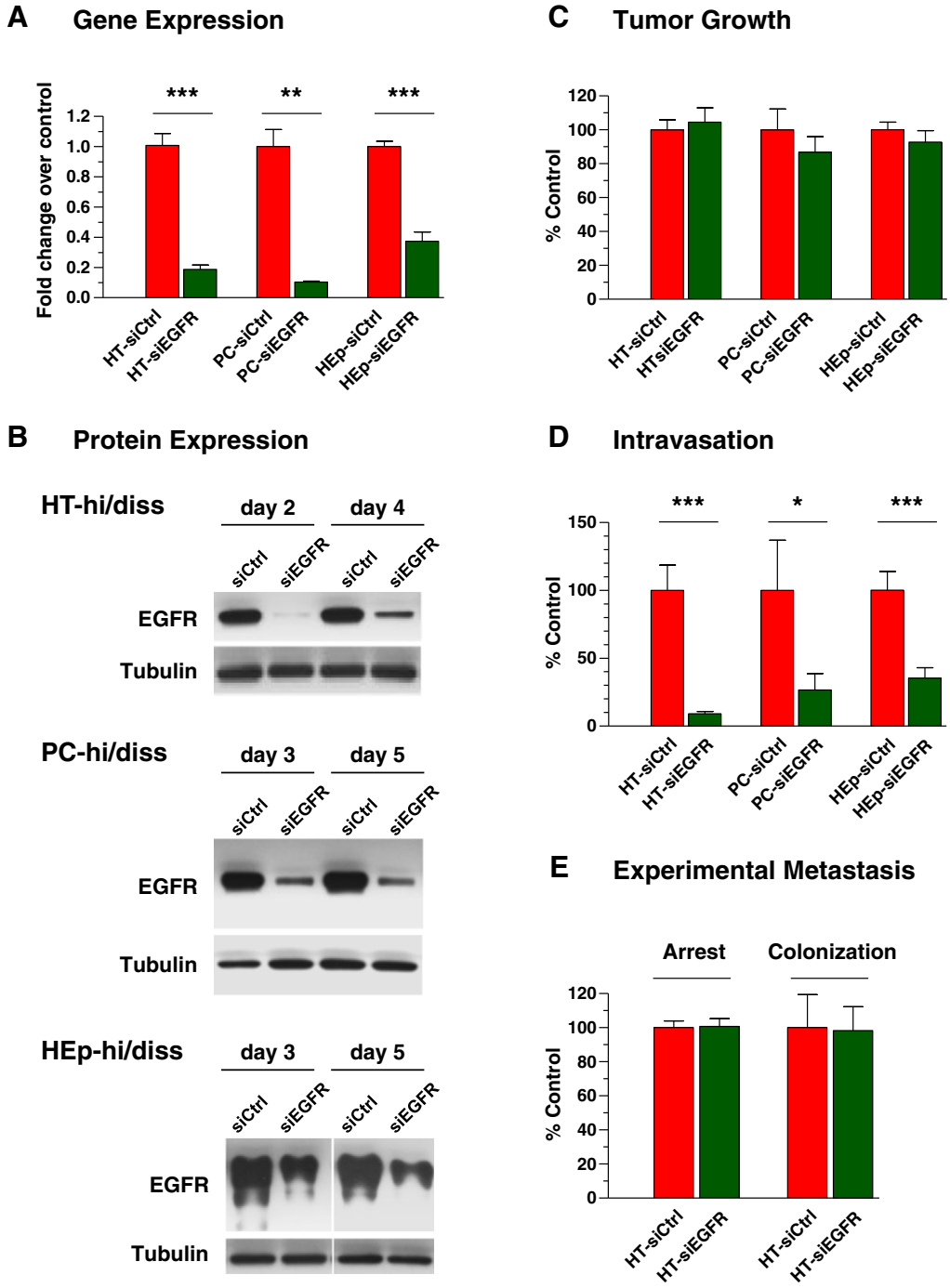

Figure 2. Functional involvement of EGFR in metastasis. Hi/diss cell variants were transiently transfected with control siRNA (siCtrl) and EGFR-specific siRNA (siEGFR). (A) Forty-eight hours after transfection, levels of EGFR gene expression were analyzed by qRT-PCR and normalized to GAPDH (1.0). Data are from two or three independent experiments for each tumor type. (B) The levels of total EGFR protein were analyzed by Western blotting from 2 to 5 days after transfections. Reprobing for tubulin provided loading control. Tumor cells transfected with siCtrl or siEGFR constructs were analyzed in spontaneous metastasis assays for tumorigenicity (C) and levels of intravasation (D). Data are expressed as the percentage of control (100%) calculated from the pooled data from two (PC-hi/diss and HEp-hi/diss variants) and four (HT-hi/diss) independent experiments. (E) HT-hi/diss cells treated with control or EGFR siRNA constructs were injected i.v. and analyzed by *Alu*-qPCR for the levels of vascular arrest at 2 hours and tissue colonization at 5 days after cell inoculations. Data are expressed as the percentage of control (100%) calculated from two independent experiments employing 14 embryos for each of control and EGFR-silenced groups.

only 21% in control microtumors (Figure 3*C*). This deficiency in 15- to 30-μm–sized intratumoral vasculature in EGFR-deficient tumors positively correlated with a significant suppression of intravasation of EGFR-silenced cells (by 72% of control) (Figure 3*D*). Importantly, Western blot analysis of excised microtumors confirmed that EGFR silencing was still sustained at the end of the 5-day-long experiment (Figure 3*E*), allowing to link the EGFR expression with tumor cell intravasation and the microarchitecture of intratumoral blood vessels.

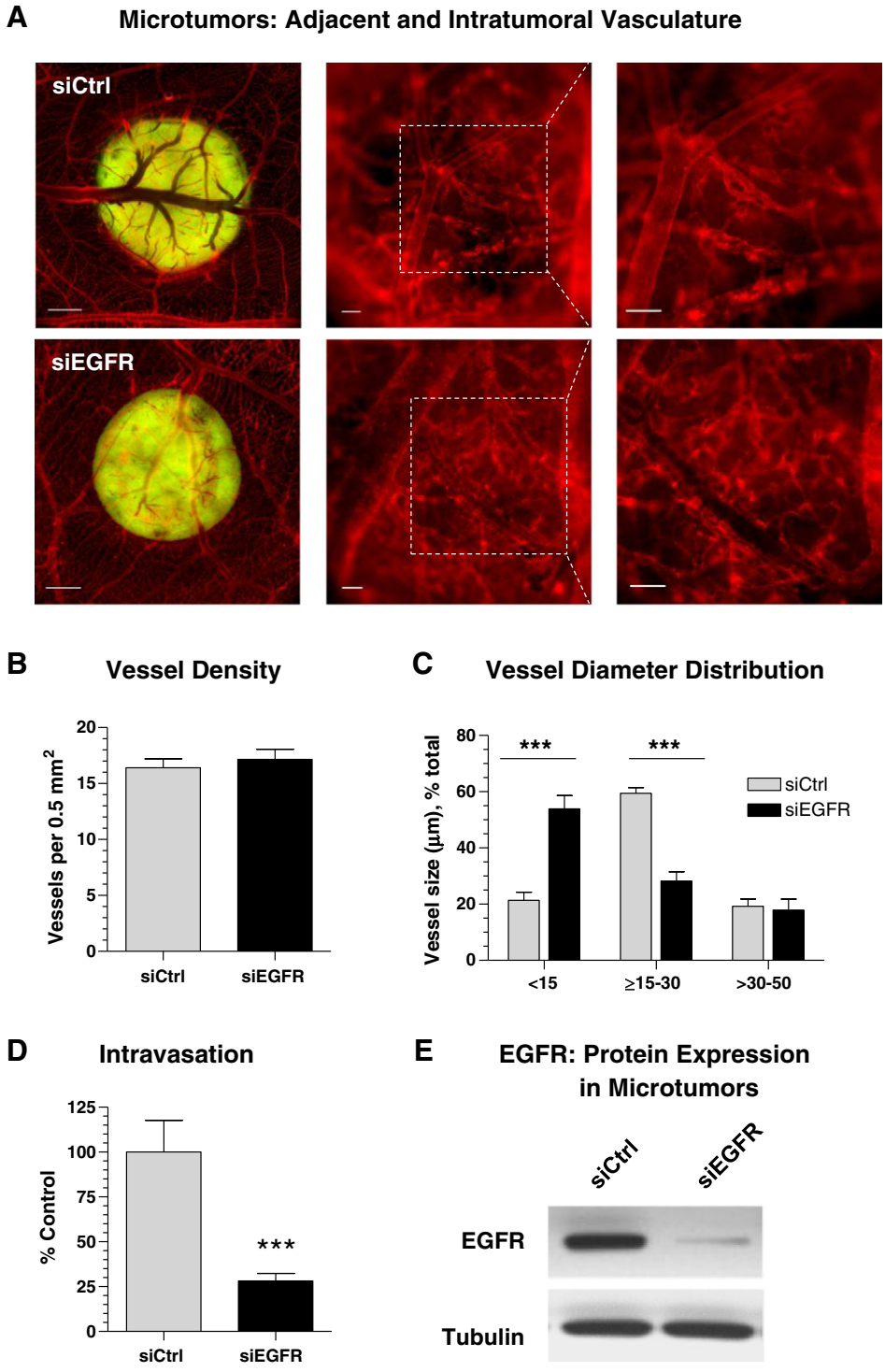

Figure 3. Tumor cell EGFR regulates the development and microarchitecture of intratumoral intravasation-sustaining angiogenic vasculature. (A) GFP-labeled HT-hi/diss cells were treated with control (siCtrl) or EGFR (siEGFR) siRNAs and grafted on the CAM of chick embryos. On day 5, the fluorescently labeled vasculature (red) was examined around and within topical microtumors (green) at an original magnification of 20× (left; bar, 1 mm), 100× (middle; bar, 100 μm), and 200× (right; bar, 100 μm). Digital images of 30 control and 25 EGFR-deficient microtumors were analyzed for the overall density (B) and lumen diameter (C) of intratumoral blood vessels. (D) Intravasation levels were quantified by *Alu*-qPCR and presented as percentage of control (100%) from three independent experiments involving 18 siCtrl-embryos and 20 siEGFR-embryos. (E) Individual microtumors were analyzed by Western blotting for total EGFR protein. Reprobing for alpha-tubulin provided a loading control.

Together, these data have highlighted a specific role of EGFR that is different from its direct effects on tumor cells and have suggested a novel mechanism whereby the activity of EGFR also produces microenvironmental cues involved in the induction and development of an intratumoral angiogenic vasculature capable of sustaining tumor cell intravasation and dissemination.

Development of Intravasation-Sustaining Vasculature and the Activity of EGFR

To analyze if the decrease in tumor cell intravasation caused by the downregulation of EGFR expression involves the suppression of downstream signaling, we inhibited EGFR tyrosine kinase phosphorylation with erlotinib. HT-hi/diss microtumors were initiated and then treated daily by topical applications of 10 µl of 30 µM erlotinib or vehicle (1% DMSO in PBS). On day 5, the embryos were injected with red fluorescent lectin to highlight the vasculature for epifluorescence microscopy. Alternatively, the microtumors were

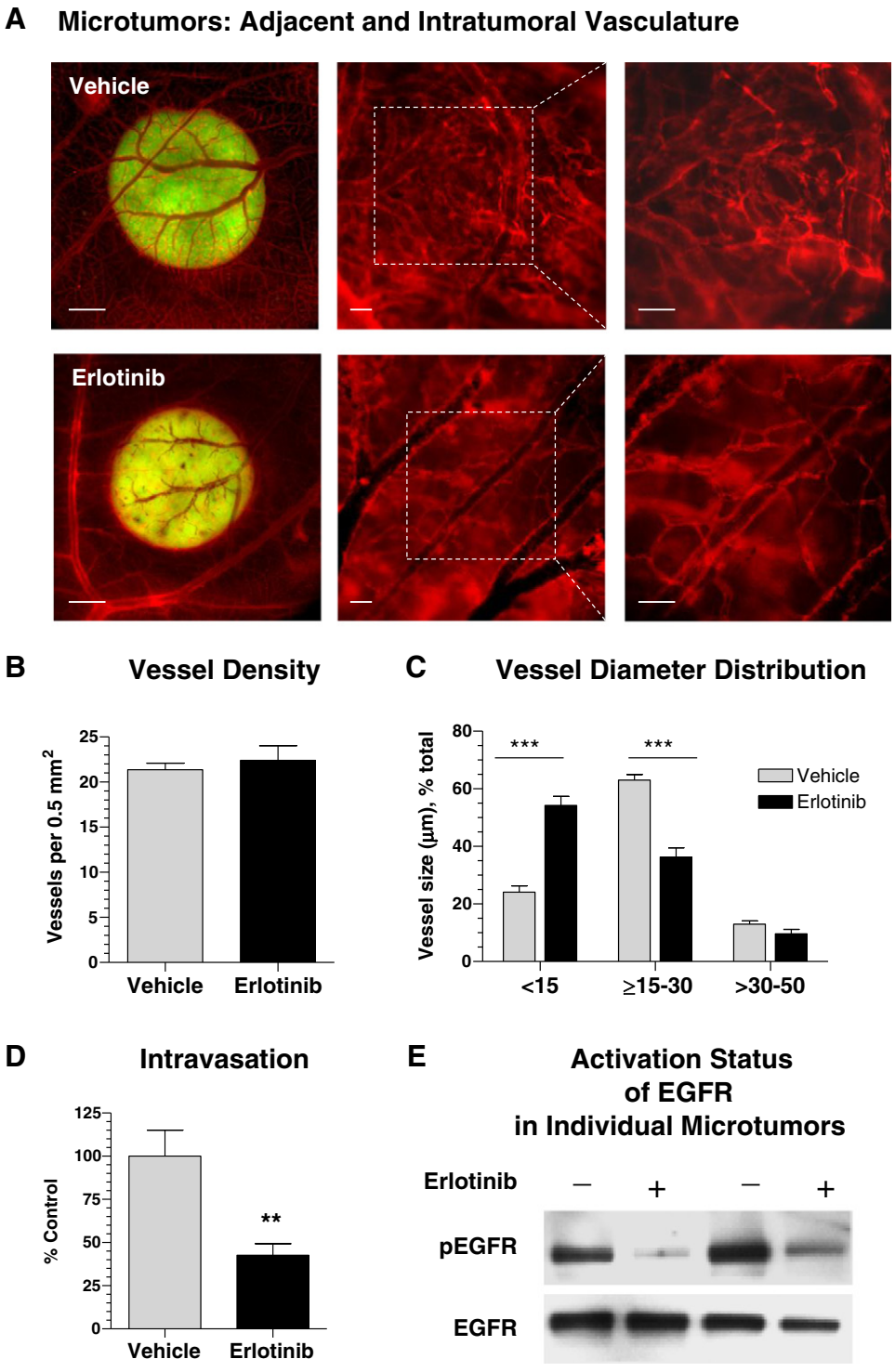

Figure 4. Development of intravasation-sustaining vasculature requires the activity of tumor cell EGFR. Microtumors developing from GFP-labeled HT-hi/diss cells were treated daily with erlotinib or vehicle and analyzed on day 5 for appearance of intratumoral vasculature (A), blood vessel density (B), and lumen diameter distribution (C) as described in Figure 3. Data are from two representative experiments employing 31 vehicle- and 24 erlotinib-treated microtumors. (D) Tumor cell intravasation was analyzed by *Alu*-qPCR in 17 vehicle- and 16 erlotinib-treated embryos. Percentage of control (100%) calculated from two pooled experiments. (E) Vehicle- and erlotinib-treated microtumors were analyzed by Western blotting for the levels of total EGFR and phosphorylated EGFR (pEGFR).

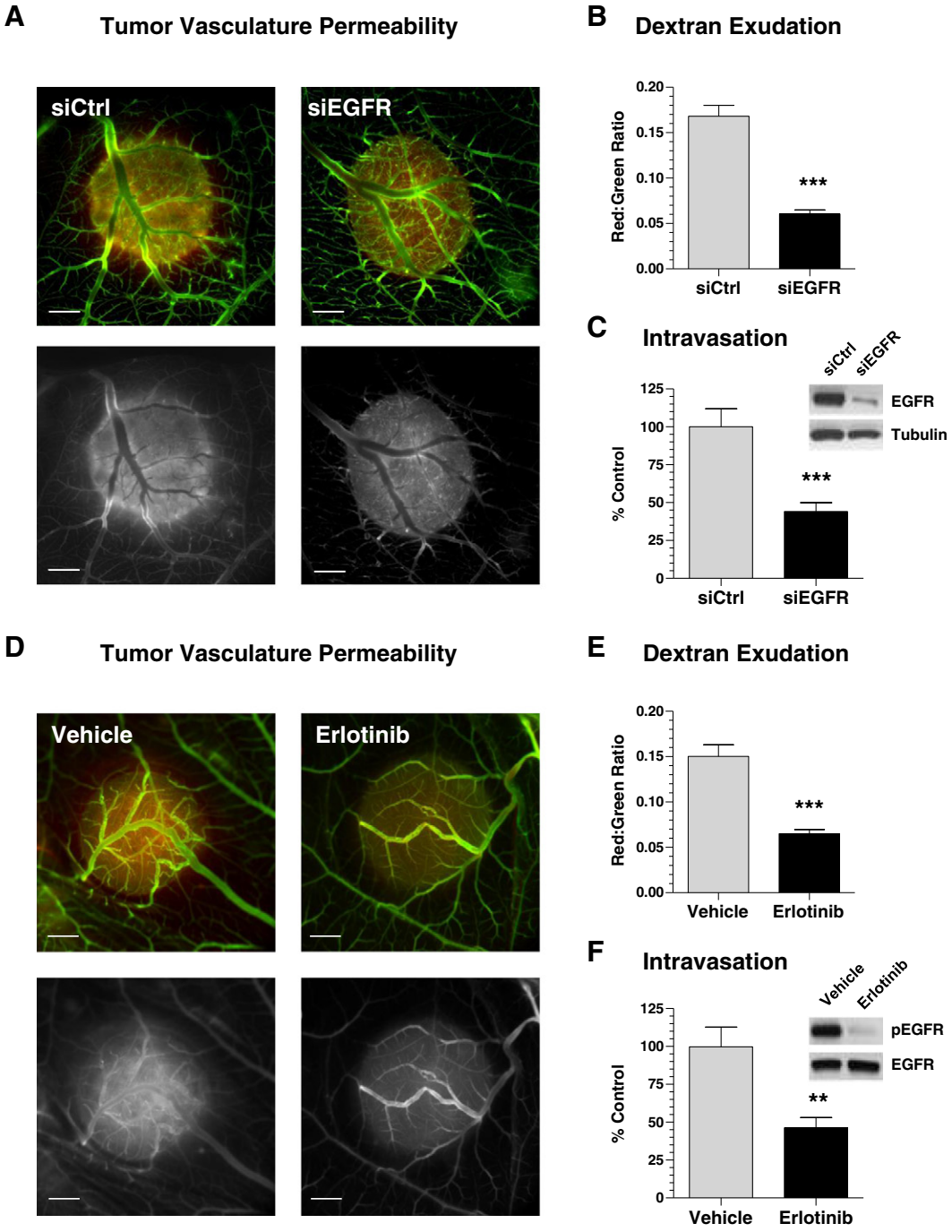

Figure 5. Tumor cell EGFR regulates the permeability of intratumoral intravasation-sustaining vasculature. (A) Microtumors were initiated from nonlabeled HT-hi/diss cells transfected with control siRNA (siCtrl) or EGFR siRNA (siEGFR). On day 5, embryos were injected with permeable TRITC-dextran. After 1 hour, embryos were inoculated with nonpermeable FITC–dextran and imaged in a fluorescent microscope (bar, 1 mm). (Top panels) Green and red fluorescence signals, representing TRITC- and FITC-dextrans, are merged. (Bottom panels) Red fluorescence is depicted monochromatically to highlight TRITC-dextran exudation. (B) Microtumors were lysed, and levels of red and green fluorescence were measured. The vascular permeability in individual tumors is presented as ratio of dextran exudation (red fluorescence) to total volume of perfusable vasculature (green fluorescence). Data are from pooled ratios from 125 siCtrl and 87 siEGFR individual microtumors. (C) Intravasation was quantified by *Alu*-qPCR from three independent experiments involving 39 siCtrl-embryos and 30 siEGFR-embryos. The data are expressed as percentage of control (100%). (Inset) Sustained downregulation of total EGFR in CAM microtumors was validated by Western blotting. (D) Microtumors were initiated from nonlabeled HT-hi/diss cells and treated with erlotinib or vehicle. Dextran permeability was visualized as described in (A). (E) Vascular permeability was quantified as described in (B). Data are from two representative experiments employing 52 vehicle- and 58 erlotinib-treated microtumors. (F) Intravasation was quantified by *Alu*-qPCR in two independent experiments involving 22 vehicle-control and 20 erlotinib-treated embryos. The data are expressed as percentage of control (100%). (Inset) Sustained inhibition of EGFR phosphorylation (pEGFR) in CAM microtumors was validated by Western blotting.

excised and analyzed by Western blotting for the levels of total and activated (phosphorylated) EGFR.

Erlotinib-mediated inhibition of EGFR activity did not prevent the convergence of tumor-adjacent blood vessels towards the border of the primary microtumors or significantly affect the overall development of tumor vasculature (Figure 4*A*). Furthermore, quantitative analysis showed no significant difference in the density of angiogenic vessels inside the microtumors (Figure 4*B*). However, the vessel size distribution analysis demonstrated a significant disproportion between control and erlotinib-treated tumors (Figure 4*C*). Thus, erlotinib substantially reduced the percentage of 15- to 30-μm–sized blood vessels compared with control group (63% vs 36%). In turn, a majority of vessels (54%) within erlotinib-treated tumors had a lumen <15 μm in diameter compared with only 24% in the vehicle-treated control (Figure 4*C*). Therefore, the development patterns of intratumoral vasculature in erlotinib-treated tumors were very similar to those observed in EGFR-silenced tumors (Figure 3). Also similar to EGFR-silenced tumors, erlotinib treatment resulted in a substantial 57% inhibition of spontaneous intravasation compared with vehicle treatment (Figure 4*D*). Importantly, whereas erlotinib did not significantly affect the total EGFR in tumors, Western blot analysis confirmed a significant inhibition of EGFR activation (Figure 4*E*).

These findings indicate that it is not just total EGFR but also EGFR downstream signaling involving tyrosine phosphorylation activation that indirectly regulates structural development of intravasation-sustaining angiogenic vasculature and, in turn, determines the levels of angiogenesis-dependent tumor cell intravasation.

Tumor Cell EGFR and Permeability of Intratumoral Angiogenic Vasculature

The demonstrated differential in blood vessel diameter distribution suggested that although EGFR positively regulates vessel dilation, it might negatively affect the integrity of endothelial layer. This suggestion is supported by highly hemorrhagic appearance of microtumors developing from control siRNA-treated cells in contrast to more benign pale-looking microtumors originating from EGFR-silenced cells (Supplementary Figure S3). To verify whether EGFR activity is responsible for increased vessel leakage, we compared *in vivo* exudation of low mol. wt. TRITC-dextran within control HT-hi/diss microtumors versus microtumors that either were generated from EGFR-silenced cells or were treated with erlotinib. Higher exudation levels of permeable dextran were detected within control microtumors (siCtrl and vehicle-treated) in contrast to either siEGFR- or erlotinib-treated tumors (Figure 5, *A* and *D*). Fluorometric quantifications confirmed that both downregulation of EGFR expression and inhibition of EGFR activity significantly reduced, by more than 50%, the levels of vascular permeability (Figure 5, *B* and *E*). Furthermore, a significant reduction in tumor cell intravasation (~55% of control) was observed along with significant downregulation of EGFR expression (Figure 5*C*) or inhibition of EGFR activation (Figure 5*F*). These vascular permeability findings indicate that tumor cell EGFR regulates the integrity of the host vasculature and, therefore, determines its ability to sustain tumor cell intravasation.

The Underlying Mechanism of EGFR-Mediated Induction and Development of Intravasation-Sustaining Angiogenic Vasculature

Induction and maturation of angiogenic vessels within primary tumors developing in the chick embryo are tightly regulated by VEGF, which becomes bioavailable after its proteolytic release from the matrix by MMP-9 that in turn, is delivered mainly by inflammatory neutrophils influxing the primary tumor in response to tumor-produced IL-8 [45,47]. Because EGFR is known to regulate the expression of many genes, including *VEGF* and *IL8* [3,49], we hypothesized that tumor cell EGFR might regulate the development of an intravasation-sustaining vasculature by controlling production of IL-8, influx of MMP-9–delivering neutrophils, and bioavailability of VEGF within the tumor microenvironment.

EGFR silencing in HT-hi/diss cells led to 85% and 50% decreases in expression of *VEGF* and *IL8* as compared with control (Figure 6*A*). Within primary tumors, this significant inhibition of gene expression was manifested in substantially reduced protein levels of soluble (bioavailable) human VEGF and also human IL-8, which correspondingly function as potent inducers of angiogenesis and chemoattractant of neutrophils in chick embryo model systems [45] (Figure 6*B*). Importantly, immunofluorescent analysis of neutrophil influx determined with a host-specific MMP-9 mAb confirmed that EGFR silencing also significantly reduced the density of MMP-9–positive neutrophils (Figure 6*B*). In the tumor microenvironment, this inflammatory cell type constitutes the major cellular source of MMP-9 [45,47,50], the protease that liberates VEGF and makes it bioavailable for angiogenesis induction [51,52]. Therefore, we have attempted to restore the diminished levels of VEGF in siEGFR-treated tumors by the exogenous delivery of purified neutrophil MMP-9. Importantly, this approach brought the levels of bioavailable VEGF in EGFR-silenced microtumors to control levels (Figure 6*B*).

To verify whether diminished levels of intravasation could be related to the VEGF and neutrophil MMP-9 deficiency caused by the downregulation of EGFR, we performed a series of *in vivo* rescue experiments in which EGFR-silenced tumors were supplemented with either purified neutrophil MMP-9 or VEGF. Daily topical applications of either purified neutrophil MMP-9 or VEGF resulted in the development of more dilated intratumoral vessels resembling those observed in control conditions (Figure 6*C*). Whereas no significant changes were observed in the overall vessel density under any test conditions (Figure 6*D*), exogenously delivered neutrophil MMP-9 or VEGF fully restored the proportion of intratumoral blood vessels with lumen sizes of 15 to 30 μm (Figure 6*E*). Importantly, this change was accompanied by a corresponding diminishment in the density of vessels of ≤15 μm in size and little or no effect on the larger, likely more mature vessels of >30 μm in diameter (Figure 6*E*). Furthermore, the siEGFR-mediated reduction of vascular permeability was also rescued by both molecular approaches (Figure 6, *F* and *G*). Finally, full restoration to control levels of tumor cell intravasation was achieved in EGFR-deficient tumors treated with either neutrophil MMP-9 or VEGF (Figure 6*H*), further demonstrating the molecular link between primary tumor cell intravasation, neutrophil MMP-9, and bioavailable VEGF

In conclusion, our findings reveal a new mechanism whereby the levels of tumor cell EGFR can ultimately determine the efficiency of tumor cell intravasation by controlling the specific microarchitecture of intratumoral angiogenic vessels through the bioavailable VEGF that is catalytically liberated by the MMP-9 released from primary tumor-attracted inflammatory neutrophils.

Discussion

Although being highly specific and potent in preclinical studies, the EGFR inhibitors are used mainly as additional lines of cancer therapy

in patients with late-stage cancers [8,13–15,53]. Mutations and amplifications of certain cancer-related genes along with acquired EGFR-activating mutations are thought to facilitate cancer resistance to EFGR-targeted therapies [5,8,9,12,16,54]. However, the relative inefficiency of EGFR inhibition even in cancers with nonmutated EGFR suggests that additional pathways could allow the EGFR-overexpressing cancer cells to escape anti-EGFR therapy. In the present study, we have demonstrated that the enhanced activity of EGFR has an important role in spontaneous dissemination of cancer cells by facilitating the development of a permeable intravasation-

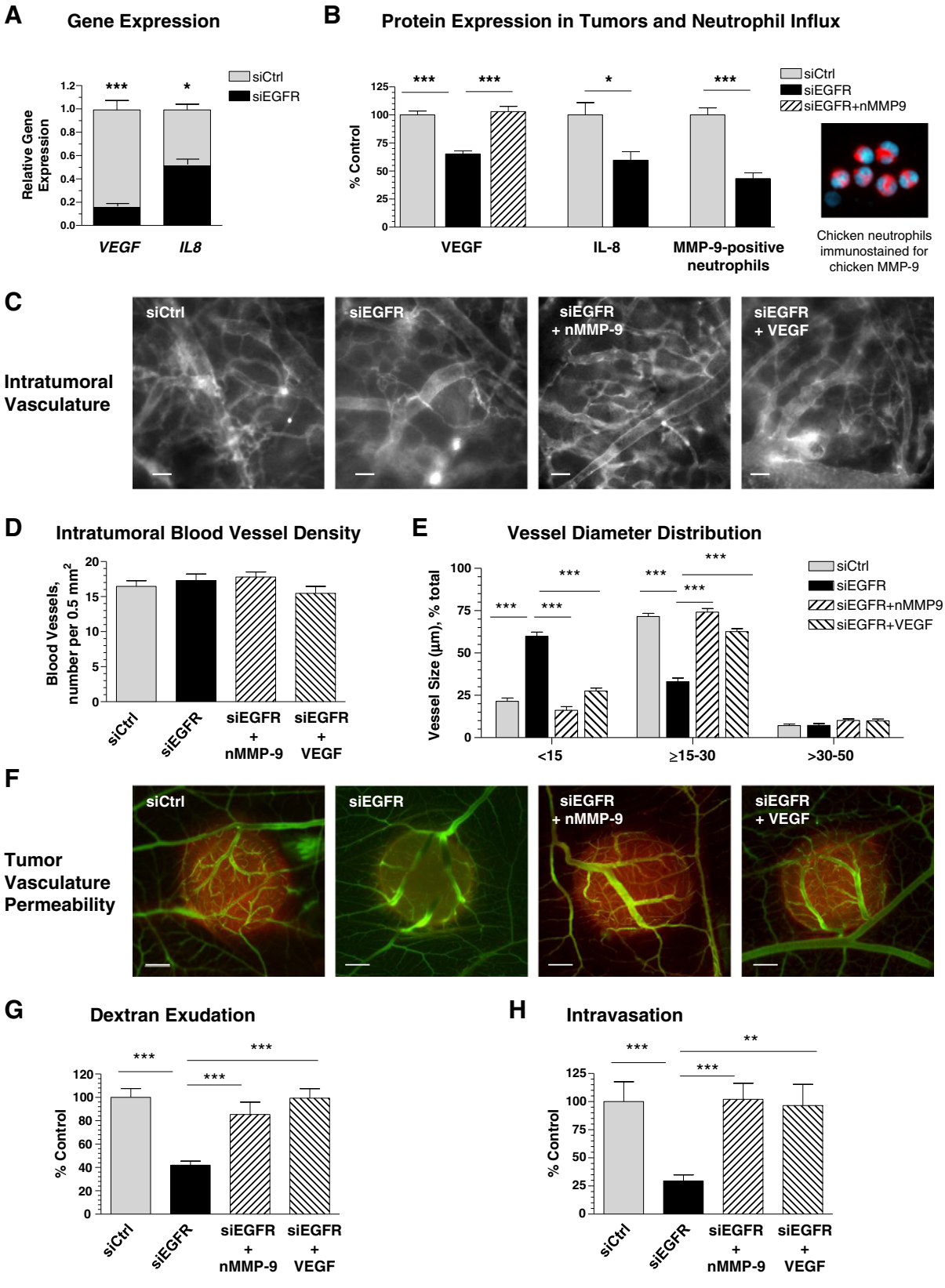

sustaining vasculature. This distinct network of intratumoral blood vessels is induced in the primary tumor microenvironment through the EGFR-mediated molecular cross talk between tumor cell–produced VEGF and IL-8 and neutrophil-delivered MMP-9. This EGFR-involving complex pathway illuminates a new function of EGFR, distinct from its direct regulation of tumor cell physiology. Several lines of evidence allowed us to interconnect the EGFR overexpressed by primary tumor cells with the capacity of the host angiogenic vasculature to sustain tumor cell intravasation.

Firstly, the high intravasation potential of three distinct tumor types, including human fibrosarcoma and two carcinomas, directly correlated with high levels of EGFR expressed in the corresponding highly disseminating variants. Secondly, the diminishment of EGFR expression in all these variants reduced intravasation levels almost to the levels of the nonintravasating counterparts, thereby suggesting that EGFR overexpression contributes to spontaneous dissemination of tumor cells through vascular routes. Importantly, cell dissemination from primary tumors of similar size was examined in our study and therefore, siEGFR-induced suppression of intravasation was not related to diminishment of tumor growth shown in other model systems [55]. Furthermore, neither vascular arrest nor tissue colonization was affected by EGFR downregulation during experimental metastasis, strongly indicating that intravasation in the primary tumor was the most likely step that was altered by EGFR silencing. These data imply a novel role of EGFR in the metastatic cascade that is distinct from its known function as a direct regulator of tumor cell proliferation, motility, stromal invasion, and tissue colonization [21,23,55–59]. Instead, our data indicate that EGFR might facilitate tumor cell dissemination by regulating specific aspects of primary tumor microenvironment. Because tumor cell dissemination critically depends on the induction of tumor angiogenesis and establishment of blood vessel networks, we investigated whether EGFR might be responsible for induction of an intratumoral neovasculature capable of sustaining tumor cell intravasation.

The notion that EGFR could be a critical regulator of intravasation-sustaining vasculature during early tumor development was investigated by using our recently established model uniquely allowing for quantification of intravasation in tandem with quantitative analyses of vascular permeability and microarchitecture in tumors treated as whole functioning micro-organs [37,38]. Herein, the functional contribution of EGFR protein and its downstream signaling activity to intravasation was interrogated by two approaches, namely, by siRNA-mediated downregulation of EGFR expression and by erlotinib-mediated inhibition of EGFR tyrosine kinase activity. These independent approaches resulted in remarkably similar patterns of intravasation inhibition, indicating that it is the *activity* of EGFR that ultimately determines the levels of tumor cell intravasation.

Specifically, silencing and inhibition of EGFR caused a dramatic difference in the microarchitecture of intratumoral vessels between the control and EGFR-downregulated or EGFR-inhibited microtumors. Whereas no significant EGFR-dependent effects were observed in the density of blood vessels converging onto primary tumors, both the downregulation of tumor cell EGFR and the inhibition of EGFR activity led to development of weak and collapsed intratumoral vessel networks. In particular, the size distribution analysis indicated that EGFR activity was critical for the dominant appearance of intermediate-sized vessels with lumen diameters between 15 and 30 μm and that presence of this particular vessel category coincided with high levels of intravasation. In fact, the reciprocal disappearance of such intratumoral vessels from EGFR-deficient tumors allowed us to delineate this distinct class of angiogenic vessels (with lumens between 15 and 30 μm in diameter) as capable of sustaining tumor cell intravasation. Noteworthy, the larger vessels (>30 μm in diameter) were not affected by EGFR modulation, indicating that these more mature or co-opted blood vessels neither respond to anti-EGFR therapy nor facilitate tumor cell intravasation. Most importantly, the altered, collapsed structure of blood vessels in EGFR-silenced or EGFR-inhibited tumors closely correlated with significantly reduced levels of tumor cell intravasation.

In addition to the microarchitecture of intratumoral angiogenic vessels, we showed that EGFR activity also regulated their permeability. Thus, high levels of dextran exudation were observed in EGFR-competent microtumors harboring mostly middle-sized vessels (≥15-30 μm), pointing to this category of intratumoral neovessels as permeable and accessible for tumor cell penetration because these vessels already posses a lumen that can readily accommodate an intravasating tumor cell but have not yet developed a hard-to-disrupt, nonleaky endothelial barrier. Decreased permeability of intratumoral vasculature was observed both in EGFR-silenced tumors and in tumors treated with EGFR inhibitor erlotinib. Whereas erlotinib can directly affect the development of angiogenic vasculature through the endothelial cell EGFR and cause vascular normalization [60], the silencing of EGFR in the primary tumor cells suggested that EGFR could modulate tumor microenvironment through regulating the production of VEGF, a critical angiogenesis inducer and important regulator of blood vessel permeability. Consistent with the EGFR-mediated regulation of *VEGF* expression and antiangiogenic effects of EGFR inhibition [23,61–63], we

Figure 6. EGFR-mediated development of intravasation-sustaining vasculature involves the tumor cell-produced VEGF released by neutrophil MMP-9. A) Gene expression of *VEGF* and *IL8* was determined by RT-qPCR in siCtrl or siEGFR HT-hi/diss cells. Data are fold difference over GAPDH levels (1.0) calculated from two independent experiments. (B) Microtumors were initiated from siCtrl and siEGFR HT-hi/diss cells. Individual siEGFR microtumors were treated daily with 10 ng purified neutrophil MMP-9 or equal volume of vehicle (10 μl). On day 5, soluble (PBS-extracted) VEGF and IL-8 were quantified in microtumor extracts by a capture ELISA. Data are percentage of control (100%) calculated from three independent experiments. The density of neutrophils was analyzed in two independent experiments by immunofluorescent staining of microtumors for MMP-9, a specific marker of MMP-9–loaded neutrophils. Image on the right depicts neutrophils isolated from the chick embryo and immunostained with mAb specific for chicken MMP-9 (pink). DAPI staining (light blue) highlights multilobed nuclei, characteristic of neutrophils. (C–G) Fraction of siEGFR microtumors was treated daily with 10 ng neutrophil MMP-9, 25 ng VEGF, or equal volume of vehicle (10 μl). On day 5, microtumors were analyzed for overall appearance of the vasculature (C), blood vessel density (D), vessel diameter (E), and tumor vasculature permeability (F and G) as described in Figures 3 and 5. Data are from three independent experiments employing eight embryos for each treatment condition (49 siCtrl tumors, 49 siEGFR tumors, 22 siEGFR tumors treated with neutrophil MMP-9, and 48 siEGFR tumors treated with VEGF). (H) Intravasation levels were quantified by *Alu*-qPCR and presented as percentage of control (100%) for each treatment condition from two independent experiments involving 14 siCtrl-embryos, 14 siEGFR-embryos, 14 siEGFR-embryos treated with neutrophil MMP-9, and 15 siEGFR-embryos treated with VEGF.

confirmed that downregulation of EGFR led to a significant diminishment of *VEGF* expression in cultured tumor cells. More importantly, these negative effects of EGFR inhibition were linked to diminishment of soluble VEGF protein within microtumors, allowing us to associate for the first time EGFR activity to the bioavailability of VEGF in the primary tumor microenvironment.

Whereas VEGF directly determines the levels of blood vessel permeability [64], the cancer cell–produced IL-8 determines the levels of inflammatory neutrophil influx into primary tumors [45,65,66]. In agreement with the negative effects of EGFR inhibition on IL-8 production [3,23], EGFR downregulation significantly reduced IL-8 gene and protein expression in primary tumors. Not surprisingly, the influx of tumor-infiltrating MMP-9–loaded neutrophils responding to their major attractant, IL-8, was also reduced. These results strongly suggest that the diminished levels of soluble VEGF in EGFR-deficient tumors might be linked to deficiency of neutrophil MMP-9, the critical proteinase that makes VEGF bioavailable by releasing it from the tumor-associated matrix [45,50,51]. This suggestion was confirmed by a rescuing approach whereby an exogenous delivery of purified neutrophil MMP-9 fully restored the levels of soluble VEGF in the EGFR-silenced tumors.

Together, our findings illuminated a complex interplay between EGFR-regulated production of VEGF and IL-8 by tumor cells and IL-8–mediated attraction of neutrophils delivering the VEGF-liberating protease MMP-9. These multifaceted relationships were validated when exogenous delivery to EGFR-deficient tumors of either VEGF or neutrophil MMP-9 fully restored the intratumoral vessel architecture and vascular permeability coordinately with the rescue of tumor cell intravasation. Furthermore, specific rescue approaches employing purified forms of components usually found in primary tumors, also corroborated our findings that the deficiency in tumor cell EGFR expression or EGFR activity modifies tumor microenvironment through diminished influx of MMP-9–delivering neutrophils and reduced bioavailability of VEGF. The insufficient

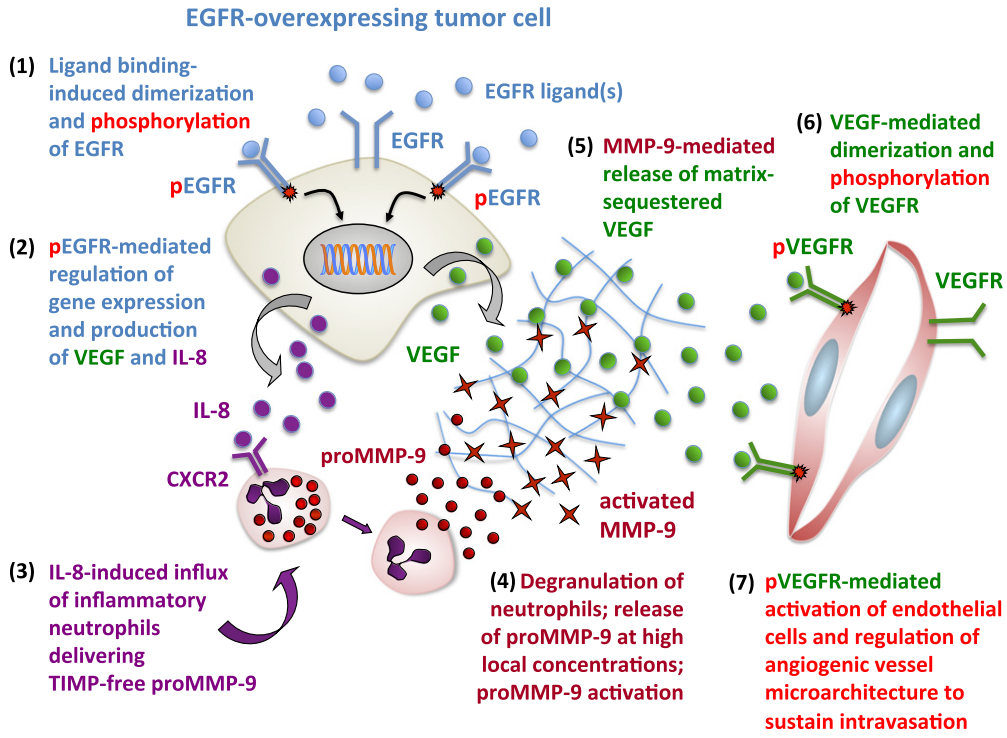

Figure 7. EGFR-mediated regulation of VEGF-dependent tumor angiogenesis. The schematic presents a mechanism whereby EGFR overexpressed on aggressive tumor cells interacts with one of its soluble ligand(s), which causes dimerization of EGFR and tyrosine phosphorylation of its cytoplasmic domain (1). Through intracellular signaling pathways, the functionally activated EGFR induces expression of many genes, including *VEGF* and *IL8* (2). Increased production of VEGF results in accumulation of matrix-bound VEGF that requires proteolytic liberation to become bioavailable and gain an angiogenesis-inducing capacity. Increased expression of IL-8 protein, the major neutrophil chemoattractant, leads to influx of inflammatory neutrophils (3) because they express high levels of CXCR2, the major receptor of IL-8. Tumor-infiltrating neutrophils, in turn, constitute the major cellular source of MMP-9, the VEGF-liberating protease. Neutrophil MMP-9 is prestored in the secretory granules as a proMMP-9 zymogen which upon neutrophil degranulation is activated by still largely unknown mechanisms that possibly involve binding of proMMP-9 to collagenous matrices (4). Activated MMP-9, which has extremely high affinity to collagenous fibrils, digests partially denatured matrix fibrils, thereby liberating matrix-bound VEGF (5). Soluble VEGF becomes a bioavailable factor capable of binding to the VEGFR on the endothelial cell, causing VEGFR dimerization and dimerization-dependent signaling (6). Activated endothelial cells then form capillaries and lumen-containing angiogenic blood vessels (7). Relatively high levels of VEGF are required for induction of lumen formation and also for the maintenance of lumen space. On the other hand, high levels of VEGF reduce the integrity of the endothelial barrier, thus assuring certain levels of endothelial layer permeability to facilitate tumor cell penetration into the inner space of an angiogenic vessel. Silencing of EGFR or inhibition of its activity would prevent the above-described chain of events, leading to detrimental conditions for development of angiogenic vasculature capable of sustaining tumor cell intravasation.

levels of bioavailable VEGF as a result of dampened levels of EGFR, IL-8, neutrophil influx, and neutrophil MMP-9 would significantly impair VEGFR-mediated activation of the sprouting endothelial cells. Consequently, this impairement would prevent formation of the angiogenic vessels with sizable 15- to 30-μm lumens, which appear to be required to provide a sufficient space for intravasating tumor cells. Alternatively, the angiogenic vessels might be formed but not be dilated enough or be permeable enough for tumor cell penetration through the endothelial cell barrier. In our study, this scenario is consistent with the observed accumulation of small-sized blood vessels in EGFR-silenced tumors and apparent insensitivity of larger, possibly co-opted vessels to diminished levels of VEGF in the tumor microenvironment. Therefore, the overall functional significance of tumor-expressed EGFR in regulation of tumor angiogenesis, vascular structure, and vessel integrity strongly implicates for the first time a specific mechanism involving EGFR in the development of a distinct intravasation-sustaining intratumoral vasculature (Figure 7).

Our study also highlights some mechanistic checkpoints, which could explain a relative inefficiency of anti-EGFR therapies. First, vascular dissemination of tumor cells responsible for metastatic disease can occur much earlier than the time frame when anti-EGFR therapy is initiated in most cancer patients. Therefore, the success of any anti-EGFR therapy might be limited to the early stages of cancer progression when EGFR inhibitors would effectively target the young, developing intratumoral vasculature, which provides the conduits for early-on primary tumor cell dissemination. In contrast, more mature vessels could be stabilized with protective pericytes that would protect the underlying endothelium from either too high or too low concentrations of VEGF [67,68]. These considerations can provide additional reasons for the modest success of anti-EGFR inhibitors used in clinic for late-stage cancer patients, whose primary tumors might have larger proportion of co-opted blood vessels that are less sensitive to diminishment of VEGF caused by EGFR therapeutics. Second, our data indicate that tumor cell intravasation could be sensitive even to moderate diminishment of EGFR-dependent production of VEGF and IL-8 proteins, IL-8–dependent neutrophil influx, and ensuing delivery of neutrophil MMP-9 releasing matrix-bound VEGF. The dependence of intravasation-sustaining intratumoral vessels on VEGF that regulates their permeability and integrity could be reflected in increased benefits of anti-EGFR therapies combined with anti-VEGF agents, a combinatorial approach currently used in clinic, albeit mainly for late-stage cancers [49,69–71]. Furthermore, our newly established mechanism suggests that additional beneficiary effects may come from combining EGFR-targeted therapy with anti–IL-8 and/or anti-inflammatory drugs [72]. These synergistic approaches could prevent the EGFR-induced delivery of MMP-9, a potent liberator of VEGF at the site of primary tumor development and a critical modulator of metastatic niches at the secondary sites [73–75]. In conclusion, the findings from this study indicate an EGFR/IL-8/neutrophil MMP-9/VEGF pathway as a valid axis to functionally compromise the intratumoral vasculature during anticancer therapy.

Acknowledgments

This study was supported by National Institutes of Health grants R01CA105412 and R01CA129484 (to J.P.Q. and E.I.D.) and the Swiss National Science Foundation for Prospective Researches (to P.M.).

The authors thank Chenxing Li for her excellent technical assistance.

Appendix A. Supplementary data

Supplementary data to this article can be found online at http://dx.doi.org/10.1016/j.neo.2015.08.002.

References

[1] Burgess AW (2008). EGFR family: structure physiology signalling and therapeutic targets. *Growth Factors* **26**, 263–274.

[2] Han W and Lo HW (2012). Landscape of EGFR signaling network in human cancers: biology and therapeutic response in relation to receptor subcellular locations. *Cancer Lett* **318**, 124–134.

[3] Ciardiello F and Tortora G (2008). EGFR antagonists in cancer treatment. *N Engl J Med* **358**, 1160–1174.

[4] Wheeler DL, Dunn EF, and Harari PM (2010). Understanding resistance to EGFR inhibitors-impact on future treatment strategies. *Nat Rev Clin Oncol* **7**, 493–507.

[5] Ohashi K, Maruvka YE, Michor F, and Pao W (2013). Epidermal growth factor receptor tyrosine kinase inhibitor-resistant disease. *J Clin Oncol* **31**, 1070–1080.

[6] Seshacharyulu P, Ponnusamy MP, Haridas D, Jain M, Ganti AK, and Batra SK (2012). Targeting the EGFR signaling pathway in cancer therapy. *Expert Opin Ther Targets* **16**, 15–31.

[7] Yu HA and Riely GJ (2013). Second-generation epidermal growth factor receptor tyrosine kinase inhibitors in lung cancers. *J Natl Compr Canc Netw* **11**, 161–169.

[8] Lo HW (2010). EGFR-targeted therapy in malignant glioma: novel aspects and mechanisms of drug resistance. *Curr Mol Pharmacol* **3**, 37–52.

[9] Pao W and Chmielecki J (2010). Rational, biologically based treatment of EGFR-mutant non-small-cell lung cancer. *Nat Rev Cancer* **10**, 760–774.

[10] Witsch E, Sela M, and Yarden Y (2010). Roles for growth factors in cancer progression. *Physiology (Bethesda)* **25**, 85–101.

[11] Baba Y, Fujii M, Tokumaru Y, and Kato Y (2012). Present and Future of EGFR Inhibitors for Head and Neck Squamous Cell Cancer. *J Oncol* **2012** [Article ID 986725, 9 pages].

[12] Ou SH (2012). Second-generation irreversible epidermal growth factor receptor (EGFR) tyrosine kinase inhibitors (TKIs): a better mousetrap? A review of the clinical evidence. *Crit Rev Oncol Hematol* **83**, 407–421.

[13] Subramaniam D, He AR, Hwang J, Deeken J, Pishvaian M, Hartley ML, and Marshall JL (2015). Irreversible multitargeted ErbB family inhibitors for therapy of lung and breast cancer. *Curr Cancer Drug Targets* **14**, 775–793.

[14] Cripps C, Winquist E, Devries MC, Stys-Norman D, and Gilbert R (2010). Epidermal growth factor receptor targeted therapy in stages III and IV head and neck cancer. *Curr Oncol* **17**, 37–48.

[15] Patel SP, Kim KB, Papadopoulos NE, Hwu WJ, Hwu P, Prieto VG, Bar-Eli M, Zigler M, Dobroff A, and Bronstein Y, et al (2011). A phase II study of gefitinib in patients with metastatic melanoma. *Melanoma Res* **21**, 357–363.

[16] Chong CR and Janne PA (2013). The quest to overcome resistance to EGFR-targeted therapies in cancer. *Nat Med* **19**, 1389–1400.

[17] Wakeling AE, Guy SP, Woodburn JR, Ashton SE, Curry BJ, Barker AJ, and Gibson KH (2002). ZD1839 (Iressa): an orally active inhibitor of epidermal growth factor signaling with potential for cancer therapy. *Cancer Res* **62**, 5749–5754.

[18] Yan Y, Lu Y, Wang M, Vikis H, Yao R, Wang Y, Lubet RA, and You M (2006). Effect of an epidermal growth factor receptor inhibitor in mouse models of lung cancer. *Mol Cancer Res* **4**, 971–981.

[19] Friess T, Scheuer W, and Hasmann M (2006). Erlotinib antitumor activity in non-small cell lung cancer models is independent of HER1 and HER2 overexpression. *Anticancer Res* **26**, 3505–3512.

[20] Li D, Ambrogio L, Shimamura T, Kubo S, Takahashi M, Chirieac LR, Padera RF, Shapiro GI, Baum A, and Himmelsbach F, et al (2008). BIBW2992, an irreversible EGFR/HER2 inhibitor highly effective in preclinical lung cancer models. *Oncogene* **27**, 4702–4711.

[21] Zhang D, LaFortune TA, Krishnamurthy S, Esteva FJ, Cristofanilli M, Liu P, Lucci A, Singh B, Hung MC, and Hortobagyi GN, et al (2009). Epidermal growth factor receptor tyrosine kinase inhibitor reverses mesenchymal to epithelial phenotype and inhibits metastasis in inflammatory breast cancer. *Clin Cancer Res* **15**, 6639–6648.

[22] Zhou W, Ercan D, Chen L, Yun CH, Li D, Capelletti M, Cortot AB, Chirieac L, Iacob RE, and Padera R, et al (2009). Novel mutant-selective EGFR kinase inhibitors against EGFR T790M. *Nature* **462**, 1070–1074.

[23] Furugaki K, Moriya Y, Iwai T, Yorozu K, Yanagisawa M, Kondoh K, Fujimoto-Ohuchi K, and Mori K (2011). Erlotinib inhibits osteolytic bone invasion of human non-small-cell lung cancer cell line NCI-H292. *Clin Exp Metastasis* **28**, 649–659.

[24] Ferrara N, Gerber HP, and LeCouter J (2003). The biology of VEGF and its receptors. *Nat Med* **9**, 669–676.

[25] Goel HL and Mercurio AM (2013). VEGF targets the tumour cell. *Nat Rev Cancer* **13**, 871–882.

[26] Kobayashi Y (2006). Neutrophil infiltration and chemokines. *Crit Rev Immunol* **26**, 307–316.

[27] Waugh DJ and Wilson C (2008). The interleukin-8 pathway in cancer. *Clin Cancer Res* **14**, 6735–6741.

[28] Tazzyman S, Lewis CE, and Murdoch C (2009). Neutrophils: key mediators of tumour angiogenesis. *Int J Exp Pathol* **90**, 222–231.

[29] Gregory AD and McGarry Houghton A (2011). Tumor-associated neutrophils: new targets for cancer therapy. *Cancer Res* **71**, 2411–2416.

[30] Piccard H, Muschel RJ, and Opdenakker G (2012). On the dual roles and polarized phenotypes of neutrophils in tumor development and progression. *Crit Rev Oncol Hematol* **82**, 296–309.

[31] Galdiero MR, Garlanda C, Jaillon S, Marone G, and Mantovani A (2013). Tumor associated macrophages and neutrophils in tumor progression. *J Cell Physiol* **228**, 1404–1412.

[32] Tazzyman S, Niaz H, and Murdoch C (2013). Neutrophil-mediated tumour angiogenesis: subversion of immune responses to promote tumour growth. *Semin Cancer Biol* **23**, 149–158.

[33] Elpek KG, Cremasco V, Shen H, Harvey CJ, Wucherpfennig KW, Goldstein DR, Monach PA, and Turley SJ (2014). The tumor microenvironment shapes lineage, transcriptional, and functional diversity of infiltrating myeloid cells. *Cancer Immunol Res* **2**, 655–667.

[34] Deryugina EI, Zijlstra A, Partridge JJ, Kupriyanova TA, Madsen MA, Papagiannakopoulos T, and Quigley JP (2005). Unexpected effect of matrix metalloproteinase down-regulation on vascular intravasation and metastasis of human fibrosarcoma cells selected in vivo for high rates of dissemination. *Cancer Res* **65**, 10959–10969.

[35] Partridge JJ, Madsen MA, Ardi VC, Papagiannakopoulos T, Kupriyanova TA, Quigley JP, and Deryugina EI (2007). Functional analysis of matrix metalloproteinases and tissue inhibitors of metalloproteinases differentially expressed by variants of human HT-1080 fibrosarcoma exhibiting high and low levels of intravasation and metastasis. *J Biol Chem* **282**, 35964–35977.

[36] Conn EM, Botkjaer KA, Kupriyanova TA, Andreasen PA, Deryugina EI, and Quigley JP (2009). Comparative analysis of metastasis variants derived from human prostate carcinoma cells: roles in intravasation of VEGF-mediated angiogenesis and uPA-mediated invasion. *Am J Pathol* **175**, 1638–1652.

[37] Juncker-Jensen A, Deryugina EI, Rimann I, Zajac E, Kupriyanova TA, Engelholm LH, and Quigley JP (2013). Tumor MMP-1 activates endothelial PAR1 to facilitate vascular intravasation and metastatic dissemination. *Cancer Res* **73**, 4196–4211.

[38] Deryugina, E. Chorioallantoic membrane microtumor model to study the mechanisms of tumor angiogenesis, vascular permeability and tumor cell intravasation. In: Angiogenesis Protocols, Third Edition. Eds. Martin SG, Hewett P. (in press).

[39] Zajac E, Schweighofer B, Kupriyanova TA, Juncker-Jensen A, Minder P, Quigley JP, and Deryugina EI (2013). Angiogenic capacity of M1- and M2-polarized macrophages is determined by the levels of TIMP-1 complexed with their secreted proMMP-9. *Blood* **122**, 4054–4067.

[40] Ossowski L and Reich E (1980). Experimental model for quantitative study of metastasis. *Cancer Res* **40**, 2300–2309.

[41] Muller PY, Janovjak H, Miserez AR, and Dobbie Z (2002). Processing of gene expression data generated by quantitative real-time RT-PCR. *BioTechniques* **32**, 1372–1374, 1376, 1378-1379.

[42] Livak KJ and Schmittgen TD (2001). Analysis of relative gene expression data using real-time quantitative PCR and the 2(-Delta Delta C(T)) Method. *Methods* **25**, 402–408.

[43] Kim J, Yu W, Kovalski K, and Ossowski L (1998). Requirement for specific proteases in cancer cell intravasation as revealed by a novel semiquantitative PCR-based assay. *Cell* **94**, 353–362.

[44] Zijlstra A, Seandel M, Kupriyanova TA, Partridge JJ, Madsen MA, Hahn-Dantona EA, Quigley JP, and Deryugina EI (2006). Proangiogenic role of neutrophil-like inflammatory heterophils during neovascularization induced by growth factors and human tumor cells. *Blood* **107**, 317–327.

[45] Bekes EM, Schweighofer B, Kupriyanova TA, Zajac E, Ardi VC, Quigley JP, and Deryugina EI (2011). Tumor-recruited neutrophils and neutrophil TIMP-free MMP-9 regulate coordinately the levels of tumor angiogenesis and efficiency of malignant cell intravasation. *Am J Pathol* **179**, 1455–1470.

[46] Bekes EM, Deryugina EI, Kupriyanova TA, Zajac E, Botkjaer KA, Andreasen PA, and Quigley JP (2011). Activation of pro-uPA is critical for initial escape from the primary tumor and hematogenous dissemination of human carcinoma cells. *Neoplasia* **13**, 806–821.

[47] Deryugina EI, Zajac E, Juncker-Jensen A, Kupriyanova TA, Welter L, and Quigley JP (2014). Tissue-infiltrating neutrophils constitute the major in vivo source of angiogenesis-inducing mmp-9 in the tumor microenvironment. *Neoplasia* **16**, 771–788.

[48] Zijlstra A, Mellor R, Panzarella G, Aimes RT, Hooper JD, Marchenko ND, and Quigley JP (2002). A quantitative analysis of rate-limiting steps in the metastatic cascade using human-specific real-time polymerase chain reaction. *Cancer Res* **62**, 7083–7092.

[49] Tabernero J (2007). The role of VEGF and EGFR inhibition: implications for combining anti-VEGF and anti-EGFR agents. *Mol Cancer Res* **5**, 203–220.

[50] Nozawa H, Chiu C, and Hanahan D (2006). Infiltrating neutrophils mediate the initial angiogenic switch in a mouse model of multistage carcinogenesis. *Proc Natl Acad Sci U S A* **103**, 12493–12498.

[51] Bergers G, Brekken R, McMahon G, Vu TH, Itoh T, Tamaki K, Tanzawa K, Thorpe P, Itohara S, and Werb Z, et al (2000). Matrix metalloproteinase-9 triggers the angiogenic switch during carcinogenesis. *Nat Cell Biol* **2**, 737–744.

[52] Ardi VC, Kupriyanova TA, Deryugina EI, and Quigley JP (2007). Human neutrophils uniquely release TIMP-free MMP-9 to provide a potent catalytic stimulator of angiogenesis. *Proc Natl Acad Sci U S A* **104**, 20262–20267.

[53] Chinnaiyan P and Harari PM (2006). Clinical advancement of EGFR inhibitors in cancer therapy. *Methods Mol Biol* **327**, 189–202.

[54] Wong KK (2008). Searching for a magic bullet in NSCLC: the role of epidermal growth factor receptor mutations and tyrosine kinase inhibitors. *Lung Cancer* **60**(Suppl 2), S10–S18.

[55] Ren W, Korchin B, Zhu QS, Wei C, Dicker A, Heymach J, Lazar A, Pollock RE, and Lev D (2008). Epidermal growth factor receptor blockade in combination with conventional chemotherapy inhibits soft tissue sarcoma cell growth in vitro and in vivo. *Clin Cancer Res* **14**, 2785–2795.

[56] Xue C, Wyckoff J, Liang F, Sidani M, Violini S, Tsai KL, Zhang ZY, Sahai E, Condeelis J, and Segall JE (2006). Epidermal growth factor receptor overexpression results in increased tumor cell motility in vivo coordinately with enhanced intravasation and metastasis. *Cancer Res* **66**, 192–197.

[57] Kedrin D, Wyckoff J, Boimel PJ, Coniglio SJ, Hynes NE, Arteaga CL, and Segall JE (2009). ERBB1 and ERBB2 have distinct functions in tumor cell invasion and intravasation. *Clin Cancer Res* **15**, 3733–3739.

[58] Dong Y, He Y, de Boer L, Stack MS, Lumley JW, Clements JA, and Hooper JD (2012). The cell surface glycoprotein CUB domain-containing protein 1 (CDCP1) contributes to epidermal growth factor receptor-mediated cell migration. *J Biol Chem* **287**, 9792–9803.

[59] Zhou ZN, Sharma VP, Beaty BT, Roh-Johnson M, Peterson EA, Van Rooijen N, Kenny PA, Wiley HS, Condeelis JS, and Segall JE (2014). Autocrine HBEGF expression promotes breast cancer intravasation, metastasis and macrophage-independent invasion in vivo. *Oncogene* **33**, 3784–3793.

[60] Cerniglia GJ, Pore N, Tsai JH, Schultz S, Mick R, Choe R, Xing X, Durduran T, Yodh AG, and Evans SM, et al (2009). Epidermal growth factor receptor inhibition modulates the microenvironment by vascular normalization to improve chemotherapy and radiotherapy efficacy. *PLoS One* **4**e6539. http://dx.doi.org/10.1371/journal.pone.0006539.

[61] Hirata A, Ogawa S, Kometani T, Kuwano T, Naito S, Kuwano M, and Ono M (2002). ZD1839 (Iressa) induces antiangiogenic effects through inhibition of epidermal growth factor receptor tyrosine kinase. *Cancer Res* **62**, 2554–2560.

[62] Ellis LM (2004). Epidermal growth factor receptor in tumor angiogenesis. *Hematol Oncol Clin North Am* **18**, 1007–1021 [viii].

[63] De Luca A, Carotenuto A, Rachiglio A, Gallo M, Maiello MR, Aldinucci D, Pinto A, and Normanno N (2008). The role of the EGFR signaling in tumor microenvironment. *J Cell Physiol* **214**, 559–567.

[64] Dvorak HF (2002). Vascular permeability factor/vascular endothelial growth factor: a critical cytokine in tumor angiogenesis and a potential target for diagnosis and therapy. *J Clin Oncol* **20**, 4368–4380.

[65] Haqqani AS, Sandhu JK, and Birnboim HC (2000). Expression of interleukin-8 promotes neutrophil infiltration and genetic instability in mutatect tumors. *Neoplasia* **2**, 561–568.

[66] De Larco JE, Wuertz BR, and Furcht LT (2004). The potential role of neutrophils in promoting the metastatic phenotype of tumors releasing interleukin-8. *Clin Cancer Res* **10**, 4895–4900.

[67] Greenberg JI, Shields DJ, Barillas SG, Acevedo LM, Murphy E, Huang J, Scheppke L, Stockmann C, Johnson RS, and Angle N, et al (2008). A role for

VEGF as a negative regulator of pericyte function and vessel maturation. *Nature* **456**, 809–813.

[68] Weis SM and Cheresh DA (2011). Tumor angiogenesis: molecular pathways and therapeutic targets. *Nat Med* **17**, 1359–1370.

[69] Argiris A, Kotsakis AP, Hoang T, Worden FP, Savvides P, Gibson MK, Gyanchandani R, Blumenschein Jr GR, Chen HX, and Grandis JR, et al (2013). Cetuximab and bevacizumab: preclinical data and phase II trial in recurrent or metastatic squamous cell carcinoma of the head and neck. *Ann Oncol* **24**, 220–225.

[70] Falchook GS, Naing A, Wheler JJ, Tsimberidou AM, Zinner R, Hong DS, Fu S, Piha-Paul SA, Janku F, and Hess KR, et al (2014). Dual EGFR inhibition in combination with anti-VEGF treatment in colorectal cancer. *Oncoscience* **1**, 540–549.

[71] Moehler M, Thomaidis T, Zeifri C, Barhoom T, Marquardt J, Ploch P, Schattenberg J, Maderer A, Schimanski CC, and Weinmann A, et al (2015). Inclusion of targeted therapies in the standard of care for metastatic colorectal cancer patients in a German cancer center: the more the better?! *J Cancer Res Clin Oncol* **141**, 515–522.

[72] Quigley JP and Deryugina EI (2012). Combating angiogenesis early: Potential of targeting tumor-recruited neutrophils in cancer therapy. *Future Oncol* **8**, 5–8.

[73] Heissig B, Hattori K, Dias S, Friedrich M, Ferris B, Hackett NR, Crystal RG, Besmer P, Lyden D, and Moore MA, et al (2002). Recruitment of stem and progenitor cells from the bone marrow niche requires MMP-9 mediated release of kit-ligand. *Cell* **109**, 625–637.

[74] Kaplan RN, Riba RD, Zacharoulis S, Bramley AH, Vincent L, Costa C, MacDonald DD, Jin DK, Shido K, and Kerns SA, et al (2005). VEGFR1-positive haematopoietic bone marrow progenitors initiate the pre-metastatic niche. *Nature* **438**, 820–827.

[75] Farina AR and Mackay AR (2014). Gelatinase B/MMP-9 in Tumour Pathogenesis and Progression. *Cancers (Basel)* **6**, 240–296.